Scientific Research Publishing

Journal of Geoscience and Environment Protection, 2022, 10, 364-384
https://www.scirp.org/journal/gep
ISSN Online: 2327-4344
ISSN Print: 2327-4336

Spatial Distribution of Soil Moisture Content and Tree Volume Estimation in International Institute of Tropical Agriculture Forest, Ibadan, Nigeria

Abiodun Akintunde Alo[1], Chukwuka Friday Agbor[2], Alice Jebiwott[3], Olubodun Temiloluwa[1]

[1]Department of Social and Environmental Forestry, University of Ibadan, Ibadan, Nigeria
[2]Department of Environmental Modeling and Biometrics, Forestry Research Institute of Nigeria, Ibadan, Oyo Nigeria
[3]Department of Social Sciences, Catholic University of Eastern Africa, Nairobi, Kenya
Email: danielakintundealo@gmail.com, chukwuka_friday@yahoo.com, aliciaphil.chebby@gmail.com

How to cite this paper: Alo, A. A., Agbor, C. F., Jebiwott, A., & Temiloluwa, O. (2022). Spatial Distribution of Soil Moisture Content and Tree Volume Estimation in International Institute of Tropical Agriculture Forest, Ibadan, Nigeria. *Journal of Geoscience and Environment Protection, 10,* 364-384.
https://doi.org/10.4236/gep.2022.108022

Received: June 30, 2022
Accepted: August 28, 2022
Published: August 31, 2022

Abstract

The role of soil moisture in the survival and growth of trees cannot be overemphasized and it contributes to the net productivity of the forest. However, information on the spatial distribution of the soil moisture content regarding the tree volume in forest ecosystems especially in Nigeria is limited. Therefore, this study combined spatial and ground data to determine soil moisture distribution and tree volume in the International Institute of Tropical Agriculture (IITA) forest, Ibadan. Satellite images of 1989, 1999, 2009 and 2019 were obtained and processed using topographic and vegetation-based models to examine the soil moisture status of the forest. Satellite-based soil moisture obtained was validated with ground soil moisture data collected in 2019. Tree growth variables were obtained for tree volume computation using Newton's formular. Forest soil moisture models employed in this study include Topographic Wetness Index (TWI), Temperature Dryness Vegetation Index (TDVI) and Modified Normalized Difference Wetness Index (MNDWI). Relationships between index-based and ground base Soil Moisture Content (SMC), as well as the correlation between soil moisture and tree volume, were examined. The study revealed strong relationships between tree volume and TDVI, SMC, TWI with R^2 values of 0.91, 0.85, and 0.75, respectively. The regression values of 0.89 between in-situ soil data and TWI and 0.83 with TDVI ascertain the reliability of satellite data in soil moisture mapping. The decision of which index to apply between TWI and TDVI, therefore, depends on available data since both proved to be reliable. The TWI surface is considered to be a more suitable soil moisture prediction index, while MNDWI exhibited a weak rela-

tionship (R^2 = 0.03) with ground data. The strong relationships between soil moisture and tree volume suggest tree volume can be predicted based on available soil moisture content. Any slight undesirable change in soil moisture could lead to severe forest conditions.

Keywords

Forest Soil Moisture, Temperature Dryness Vegetation Index, Spatial Data, Vegetation Indices

1. Introduction

Forest Soil moisture content (SMC) is one of the important environmental factors that affect natural ecosystems (Briggs, 2016). Soil is the most treasured non-renewable natural resource on earth and the most diverse part of the biosphere. Knowledge of soil moisture plays a crucial role in the field of hydrology (Bai et al., 2020; Gruhier et al., 2008), meteorology, climatology, ecology, land surface modeling, and studies in environmental changes (Gruhier et al., 2008; Verstraeten et al., 2006). Soil moisture content in forest ecology is influenced by the existing forest species, altitude, climatic conditions, density, age, and soil conditions (Briggs, 2016). According to Zwartendijk et al. (2017), the physico-chemical and biological soil properties such as temperature, ventilation, microbiological soil activity, nutrient uptake capacity, and accumulation of toxic substances are influenced indirectly by SMC. Xu et al. (2006), determined the contributions of soil water to forest biomass and the results of their study revealed a strong relationship between these ecological components.

Soil moisture is often expressed spatially as indices and such indices used include the Topographic Wetness Index (TWI), The Temperature-Vegetation Dryness Index (TVDI) and modified normalized soil water index (MNDWI) (Haas, 2010; Maselli & Chiesi, 2007; Seelig et al., 2008). The TWI was first developed in 1979 by Beven and Kirkby. It is based on surrounding topography and describes the proclivity of an area to become water-saturated. Remote Sensing based soil moisture retrieval has been a promising research field since the early 1970s. Sandholt et al. (2002), developed the TVDI that describes the relations between measured land surface temperature, vegetation and soil moisture, which could be expressed by the "triangle" method (Haas, 2010). These indices have shown to be reasonable estimators of surface soil moisture, although some questions of validity remained. However, there seems to be limited knowledge about soil moisture index-tree volume correlations and if one particular index can be considered to give superior results in the region of interest.

Accurate estimation of soil moisture content is crucial for planning and management of water resources, particularly in forest ecosystems where water is a major resource. However, information on the spatial distribution of the soil

moisture content in the study area is very limited. Therefore, this study focused on the assessment of soil moisture distribution in the International Institute of Tropical Agriculture forest, Ibadan with a view to ascertain the impact of the soil water content on tree volume as well as determining the best index for estimating soil moisture content in the study area.

2. Materials and Method

2.1. Study Area

The forest reserve, as shown in Figure 1, is located within the International Institute of Tropical Agriculture (IITA) in Akinyele local government area, Ibadan, Oyo State, south-west Nigeria. It lies between Latitudes 7˚30'14.09"N and 7˚28'55.51"N and Longitudes 3˚52'44.49"E and 3˚53'45.50"E. The forest covers an area of about 450 ha. The climate of IITA is tropical with distinct wet and dry seasons and a mean minimum annual temperature of 21˚C with seasonal variations in radiation, sunshine and cloud cover. Between March and October, the prevailing wind in the area is the moist maritime South-west monsoon which blows inland from the Atlantic Ocean, this is the period of the rainy season. November to February is the period of the dry season when the dry dust-laden wind blows from the Sahara desert. The mean annual rainfall of about 1205 mm, falling in approximately 109 days with two rainfall peaks in June and September

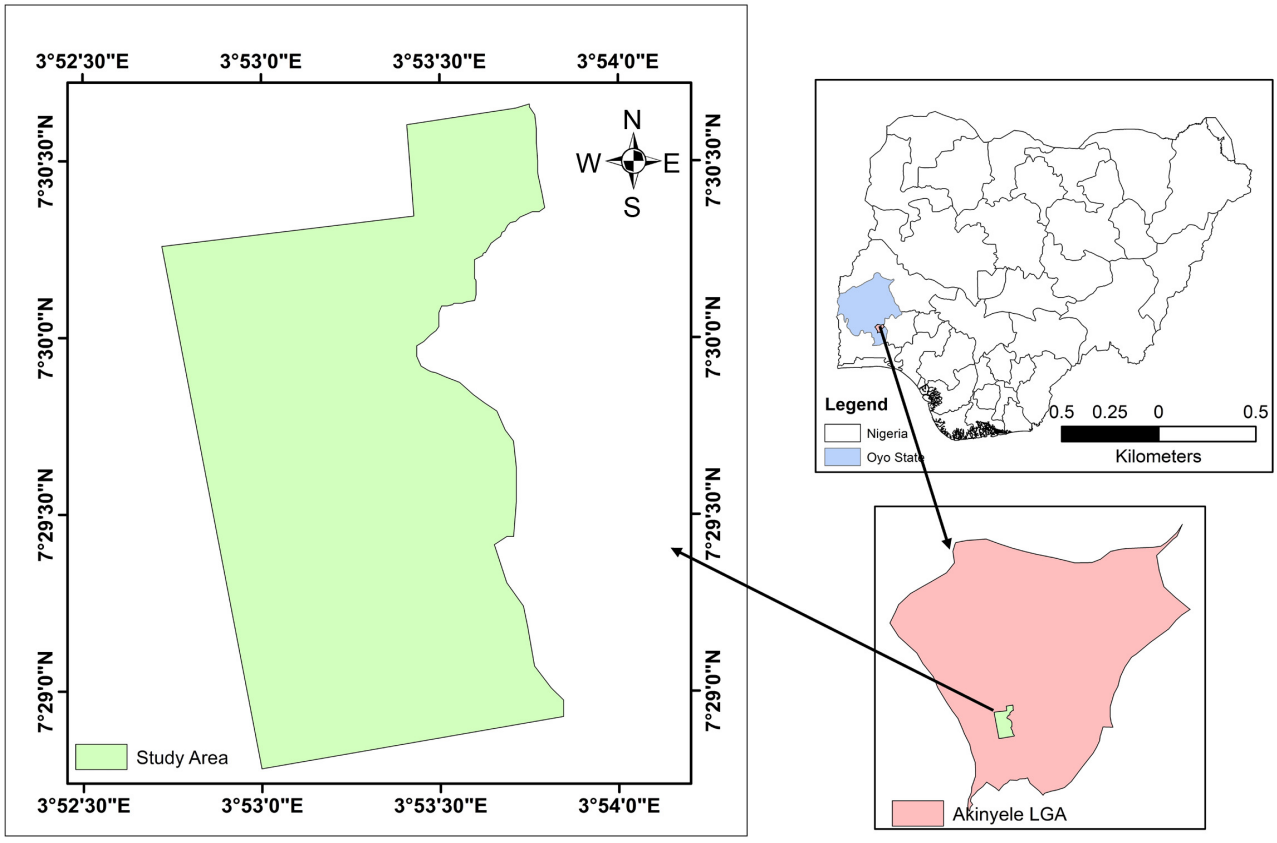

Figure 1. International institute of tropical agriculture forest, Ibadan (Source: *Protected area of Nigeria*).

(Egbinola & Amobichukwu, 2013). It is characterized by surface elevation between 160 m and 240 m above sea level, with a rainforest vegetation type.

2.2. Data Collection

Since there are no permanent sample plots in the IITA forest, temporary sample plots were adopted for this study as was done by Akindele (1991), Alo & Aturamu (2014), Alo et al. (2017), Alo et al. (2011), and Onyekwelu et al. (2003). Two transects were laid in the forest at 300 m apart. In order to account for the same dimension with the 30 m resolution of Landsat images, six 30 m by 30 m temporary sample plots were laid alternatively on each transect with an interval of 150 m for tree growth variables measurement, making a total of 12 temporary sample plots. Tree growth variables obtained from each sample plot collection were limited to; dbh of all trees encountered in the sample plot with dbh ≥ 10 cm, diameters over bark at the base, middle and merchantable top, as well as total height of the trees with the use of Spiegel Relaskop.

Landsat images of 1989, 1999, 1999, and 2019 were downloaded from the official website of US Geological Survey (USGS). The study area is within Landsat path 191 and row 55. **Table 1** shows the specifications of AsterDem, Landsat TM, ETM+ and OLI images used.

Soil samples were collected with the use of a soil core sampler at every angle and middle of each sample plot, so to achieve a good mixture of the overall soil sample of each plot. The data sets in **Table 1** were used as inputs to the ArcGIS and Idrisi software. Model setup includes delineation of the study area, topographical modeling from Asterdem, vegetation indexes from Landsat images, and index-ground data comparison (Haas, 2010). The primary and secondary data were acquired and used for this study. The primary data collected were soil and biomass data from samples plots in the field, point coordinates to identify different sample locations for effective data modeling and comparison. The coordinates were collected using hand-held Global Positioning System (GPS) of a 3m accuracy level. The secondary data include the administrative map of Nigeria collected from Remote Sensing and GIS laboratory in Forestry Research Institute of Nigeria (FRIN) and base map of the area.

Soil samples were taken from five locations of each plot at 30 cm depth by using a soil core sampler. The five soil sub-samples were bulked together to make a composite soil sample for each plot. The moist soil samples were first sieved

Table 1. Data used for the analysis.

Satellite Sensor	Spatial resolution	Acquisition years	Path/Row
Landsat 5, 7 and 8	30 m × 30 m	1989, 1999, 2009 and 2019	191/55
Asterdem	30 m × 30 m	2009	191/55

through 10 mm mesh to remove gravel, small stones and coarse roots and, then, passed through a 2 mm sieve. The initial weight of the soil sample was determined by the use of a weighing scale balance, soil samples were subjected to heat at a constant temperature of 105˚C for 24 hours. Therefore percentage soil moisture content was calculated in the following;

$$\text{MC} = \frac{\text{Initial Weight} - \text{Final Weight}}{\text{Initial Weight}} \times 100 \quad (1)$$

MC = Moisture Content.

2.2.1 Soil Moisture Retrieval in Remote Sensing

With readily available long-term remote sensing records and progress in digital image processing techniques as well as the tendency towards macro-scale modeling, remote sensing can provide large-scale distributed data sets where ground-based measurements are unavailable (Makinde & Agbor, 2019). Attempts have been made to combine remote sensing and hydrologic modeling (Bauer et al., 2006; Houser et al., 1998; Milly & Kabala, 1985). Studies have been carried to compare remotely sensed and simulated soil moisture over a heterogeneous watershed and found both techniques to be consistent with ground measurements (Haas, 2010). Soil moisture retrieval with remote sensing techniques can be achieved in all regions of the electromagnetic spectrum. Comprehensive comparisons between different retrieval techniques can be found in Bryant et al. (2003) and Moran et al. (2014). In the same vein, Haas (2010) reported soil moisture retrieval techniques and analysed their capabilities, advantages and disadvantages. The following methods mentioned have been successfully used to model soil moisture and are briefly described:

2.2.2. Dryness Index (TVDI)

Studies have revealed that remotely sensed surface temperature as measured by thermal infrared (TIR) emissions and vegetation index has a strong relation with surface soil moisture (Zhang et al., 2007; Naira et al., 2007; Sandholt et al., 2002; Wang et al., 2007; Zeng et al., 2004). The relationship has proved to be important in obtaining further information. For instance, Nemani and Running (1989) and Price (1990) were the initial studies that made use of the temperature/vegetation relationship to estimate evapotranspiration. Numerous investigations regarding the validity of the relationship have been made and modifications to improve soil moisture estimates have also been tested (Carlson, 2007; Hassan et al., 2007; Kimura, 2007). The approach of a simplified land surface dryness index, often referred to as the "triangle" method was chosen in this study (Haas, 2010). It interprets the Ts/FCD space in terms of surface soil moisture status and is based on the assumption that remotely sensed surface temperatures are related to vegetation canopy cover. The TVDI was calculated with Equation (2):

$$\text{TVDI} = \frac{T_s - T_{s\min}}{a + b_{fcd} - T_{s\min}} \quad (2)$$

where T_s = surface temperature;

T_{smin} = minimum surface temperature;

b_{fcd} = coefficient of vegetation index;

a = the intercept.

The dry edge was developed from Equation (3)

$$T_s = a + b_{fcd} \tag{3}$$

T_s = surface temperature

a, b define the parameters defining the dry edge of the triangle

The forest canopy density fcd was derived using Equation (4)

$$\text{FCD} = \sqrt{\text{SVD} * \text{SSI} + 1} - 1 \tag{4}$$

where SVD represents scaled vegetation index and SSI is the scaled shadow index calculated using a linear transformation function from normalized Advance vegetation index (AVI), Shadow index (SI) and Bare soil index (BI) (Agbor & Makinde, 2018).

The surface dryness index known as the "triangle" method as proposed by Sandholt et al. (2002) was used in this study to interpret the Ts/Fcd space in terms of forest canopy status. Sandholt et al. (2002) adopted NDVI as the vegetation index, but this study used FCD instead because NDVI is unable to highlight subtle differences in canopy density (Agbor et al., 2017).

2.2.3. Topographic Wetness Index (TWI)

The DEM was resampled to match the dimensions of Landsat images The DEM is the basis for TWI calculation and therefore requires the removal of spurious sinks and pits. TWI surface generation was performed using Equation (5) (Haas, 2010).

$$\text{TWI} = \text{Ln}\left(\left(\text{"FlowAcc\_1"} * 30\right) \Big/ \left(0.00565 + \text{Tan}\left(\text{"Slope"}/57.29\right)\right)\right) \tag{5}$$

where Ln = natural log;

FLOWACC = flow accumulationl

2.2.4. Modified Normalized Difference Water Index

The assessment of water status of vegetation canopies from spectral remote sensing data is a major goal in ecology and agriculture. Over the past decades, various studies have assessed whether soil water status, defined by leaf water content or canopy water content, can be measured using light reflected from leaves (Equation (6)) (Rokni et al., 2014).

$$\text{MNDWI} = \frac{R_{860} - R_{1240}}{R_{860} + R_{1240}} \tag{6}$$

where R_{860} and R_{1240} denote reflectance at 860 nm and 1240 nm, respectively (Komeil et al., 2014).

2.2.5. Surface Classification

In order to explore the distribution of soil moisture content in the area, the TWI,

MNDWI and TVDI surfaces were classified into five categories of very low, low, medium, high and very high values. Natural breaks classification was used here as there is no optimum classification method and the optimum number of classes for comparing the surfaces because of their unequal value distribution. The natural breaks classification after Jenks (Haas, 2010) distributes values into classes according to their natural breaks. This however means that values classified by a natural break in one surface do not belong to a natural break in the other surface. The natural breaks classification result in different category boundaries as can be seen in Figures 2-11.

2.3. Data Validation

The sample points were compared to the corresponding pixel values from the generated surfaces using the regression analysis tool in SPSS. The SPSS was used to perform linear regression analysis by using the "least squares" method to fit a line through a set of observations. It explains how a single dependent variable is affected by the values of one or more independent variables. For example, it analyzes how tree volume is affected by soil moisture level. It also explains in this

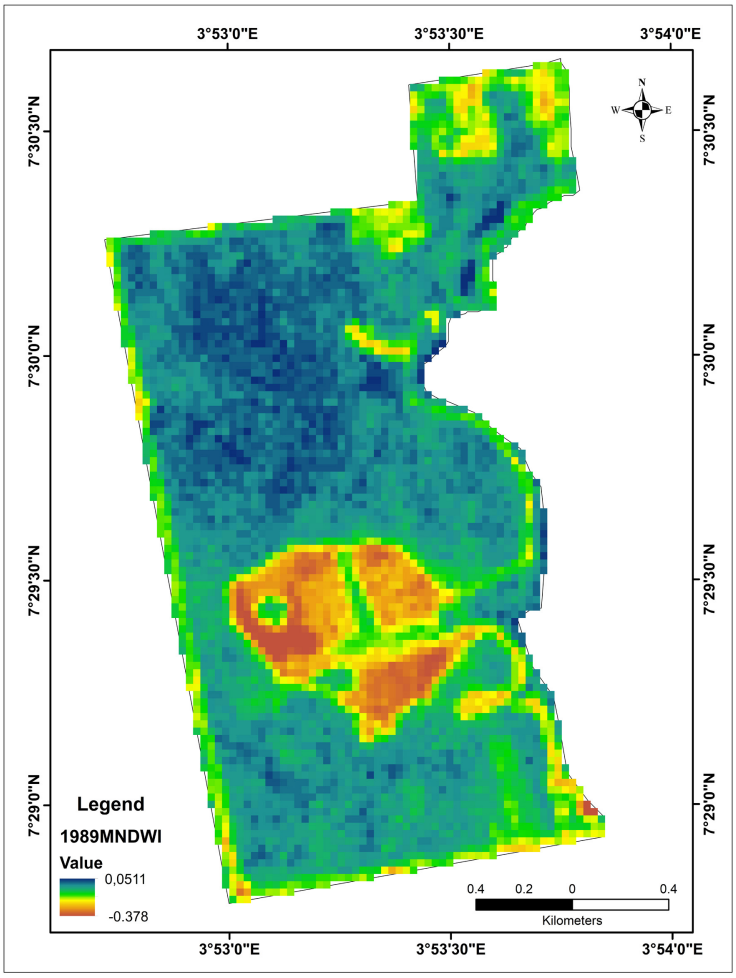

Figure 2. 1989 MNDWI.

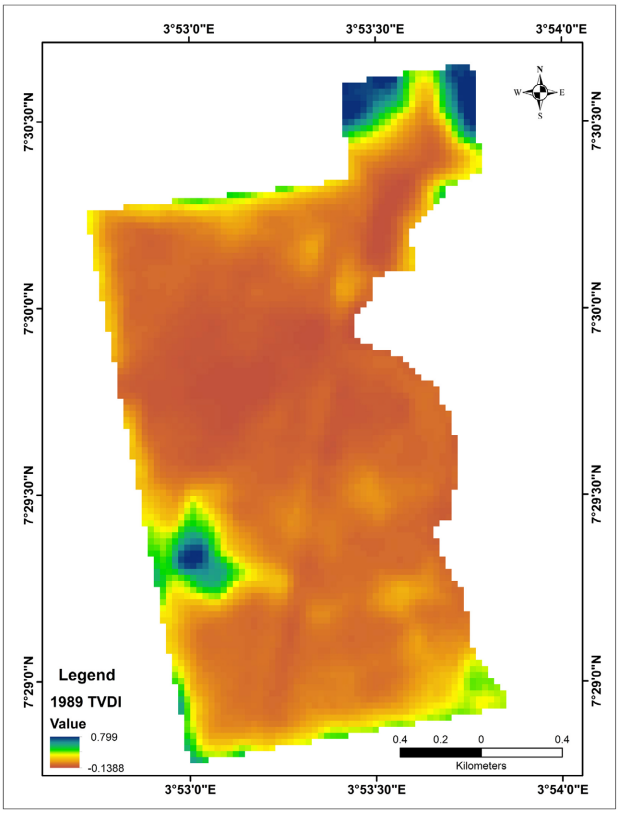

Figure 3. 1989 TVDI.

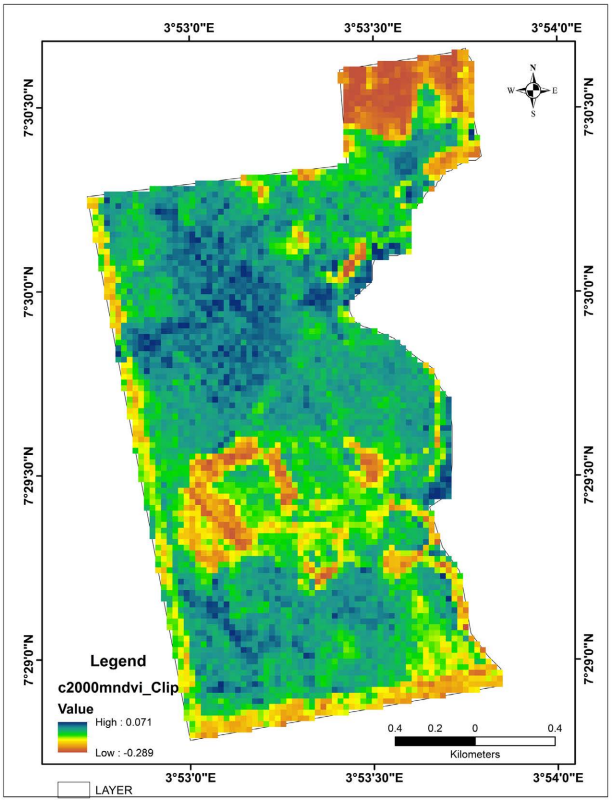

Figure 4. 1999 MNDWI.

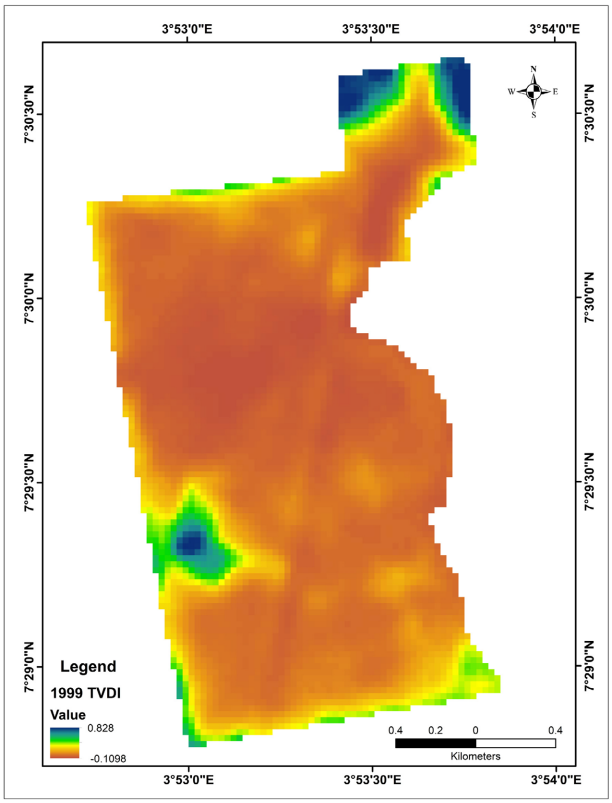

Figure 5. 1999 TVDI.

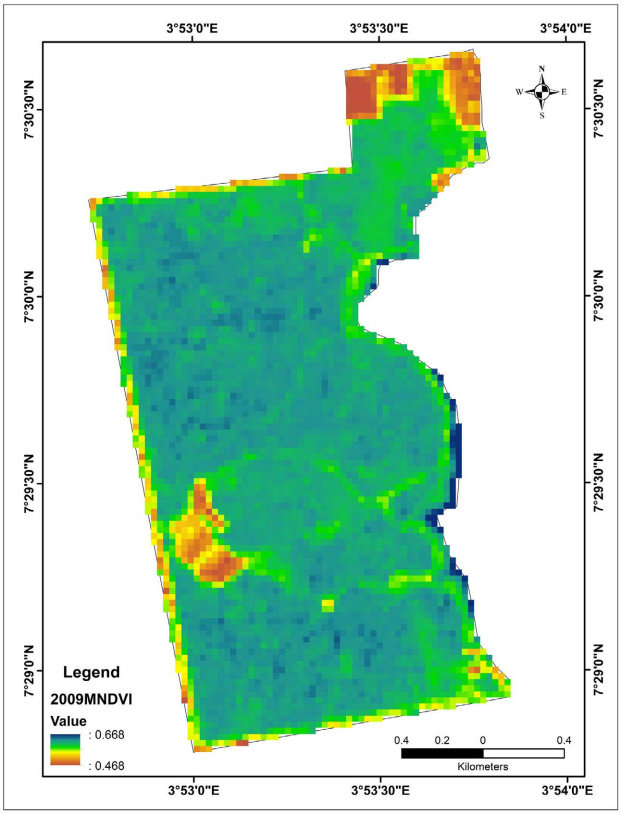

Figure 6. 2009 MNDWI.

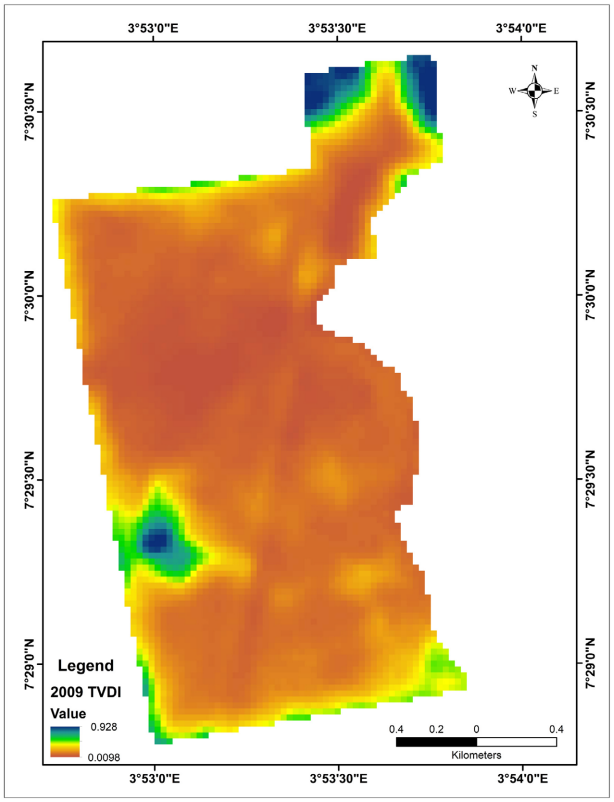

Figure 7. 2009 TVDI.

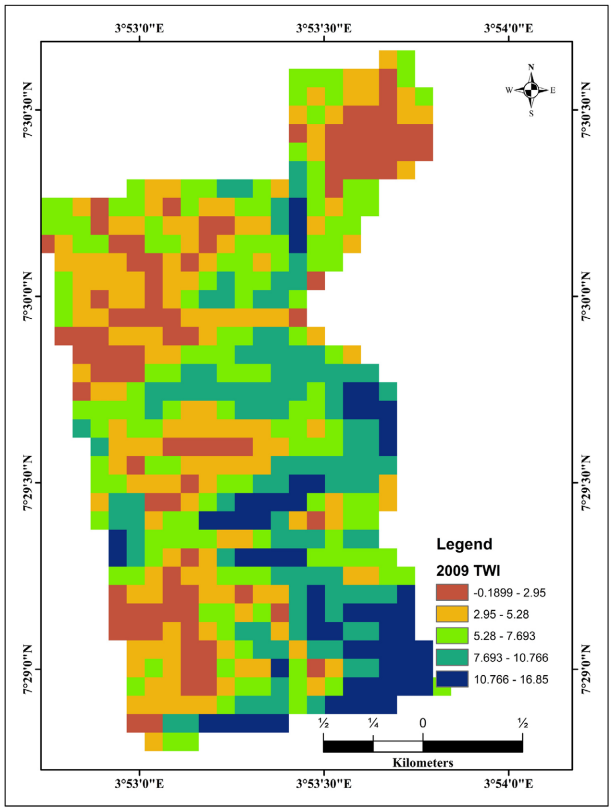

Figure 8. 2009 TWI.

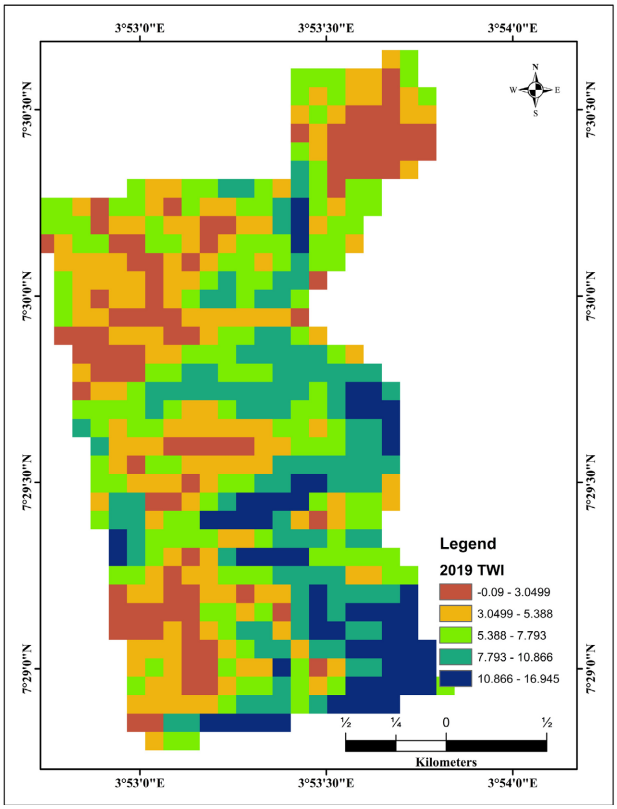

Figure 9. 2019 TWI.

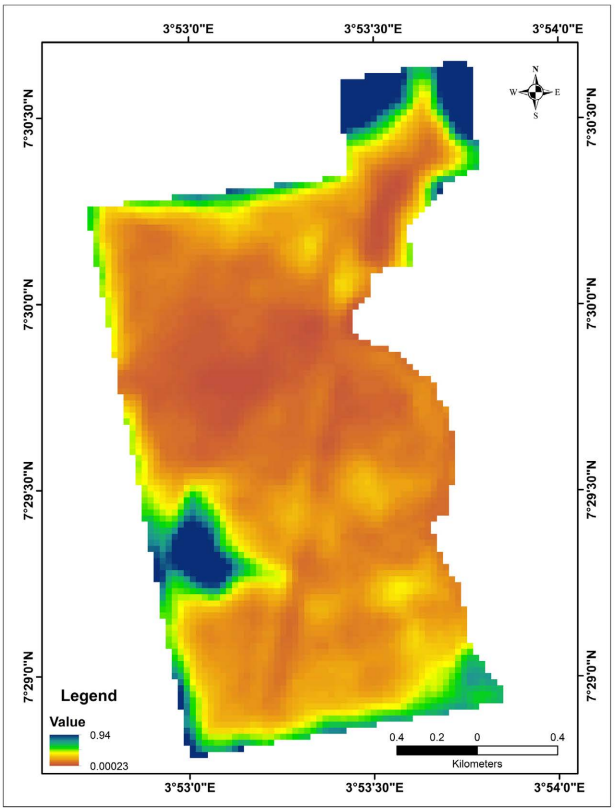

Figure 10. 2019 TVDI.

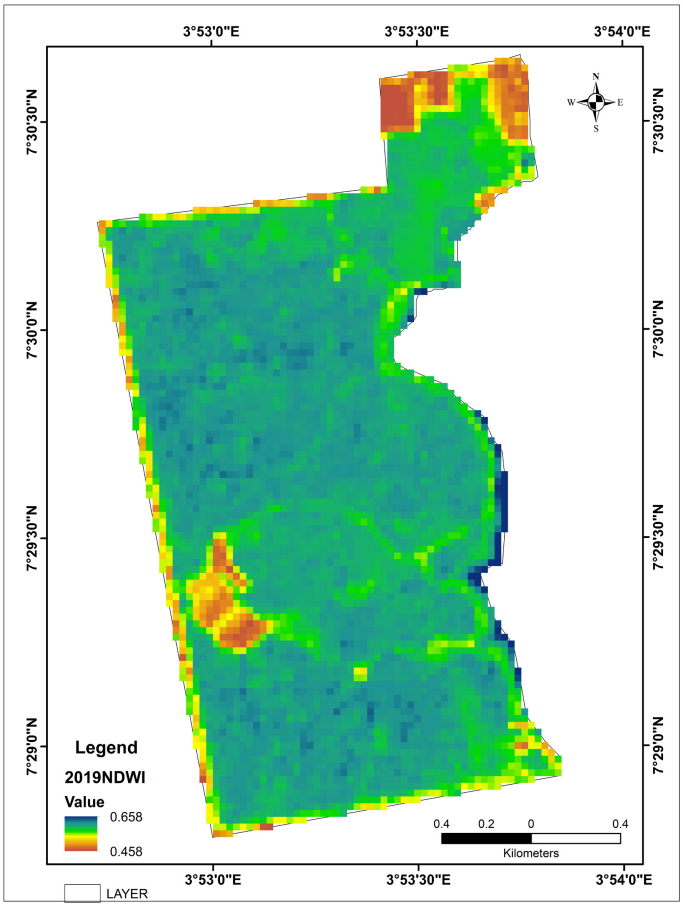

Figure 11. 2019 MNDWI.

study how closely measured soil moisture relates to the satellite-based soil moisture level. The linear regression equations (**Figures 2-11**) output the regression coefficients for each of the independent variables and the intercept. The intercept is the value for the dependent variable (e.g. tree volume) when the independent variable is zero. The coefficients indicate the effects of the independent variable on the dependent variable (soil moisture). To check if the results are reliable (statistically significant), we looked at the Significance *f* values if they are less than 0.05. The result is accepted when the F value is less than 0.05 and rejected if greater than 0.05.

2.4. Image Processing

In raw remote sensing data, each pixel has digital number value that corresponds to a raw measurement required by the sensor (Giannini et al., 2015). To obtain quantitative information from images, there is a need to convert images from their raw state to reflectance measures, using Equation (7) (Chander et al., 2009).

$$\rho\lambda = \frac{\pi \cdot \mathrm{TOAr} \cdot d^2}{E_{\mathrm{SUN}}\lambda \cdot \cos\theta_{\mathrm{sz}}} \tag{7}$$

where:

$\rho\lambda$ = Planetary TOA reflectance (unitless);

π = mathematical constant approximately equal to 3.14159 (unitless);

$L\lambda$ = Spectral radiance at the sensors aperture [w/(m^{2}sr μm)];

d^2 = The Earth-Sun distance (Astronomical unit);

E_{SUN} = Meanexo atmospheric solar irradiance [w/(m^{2}sr μm)];

θ_{SZ} = the solar zenith angle (degree). The cosine of this angle is equal to the sine of the sun elevation θ_{SE}. therefore, $\theta_{SZ} = 90 - \theta_{SE}$. These are rescaling factors given in the metadata.

2.4.1. Temperature Retrieval

All the image bands are quantized as 8-bit data except Landsat 8 which is 16 bit, thus; all information is stored in DN which will then be converted to radiance with a linear Equation (8). The linear Equation (8) (Giannini et al., 2015; Makinde & Agbor, 2019) is given as:

$$Y = mx + b \tag{8}$$

where

Y = TOAr (Top of Atmosphere) radiance—the radiance measured by the sensor;

m = Radiance multiplicative value;

x = Raw band;

b = Radiance additive value.

By applying the inverse of the Planck function, thermal bands' radiance values will be converted to brightness temperature values using Equation (8) (Agbor & Makinde, 2018).

$$B_t = \frac{K_2}{\ln\left(\frac{K_1}{\text{TOAr}} + 1\right)} - 273.15 \tag{9}$$

where

B_t = Kelvin;

TOAr = Top of Atmosphere radiance;

K_1 = calibration constant 1 (607.76 for TM), (666.09 for ETM+) and (774.89 for OLI band 10);

K_2 = calibration constant 2 (1260.56 for TM), (1282.71 for ETM+) and (1321.08 for OLI band 10).

2.4.2. Tree Volume Estimation

The volume of the trees was calculated using a common formula for volume computation, which includes; Newton's, Huber's, and Smalian's formulae of volume computation. The volume obtained with formulae were compared with volume obtained by summing up all the bolt of each felled tree for significant differences using SPSS 10.0 for window

- *Newton's formula* (Avery & Burkhart, 1983)

$$V = \frac{h}{6}\left(A_b + 4A_m + A_t\right) \tag{10}$$

where V = tree volume (m^3);

h = total height of the tree (m);

A_b = Area at the base (m^2);

A_m = Area at the middle (m^2);

A_t = Area at the top (m^2).

3. Results and Discussion

3.1. Soil Moisture Distribution and Impacts on Tree Volume

Results of the soil moisture calculated with varying settings as previously described are shown in Figures 2-11. The presentation of soil moisture distribution in sub-pixels form is to establish the relationships between soil moisture from different models and calculated forest volume. Figures 12-17 describe the

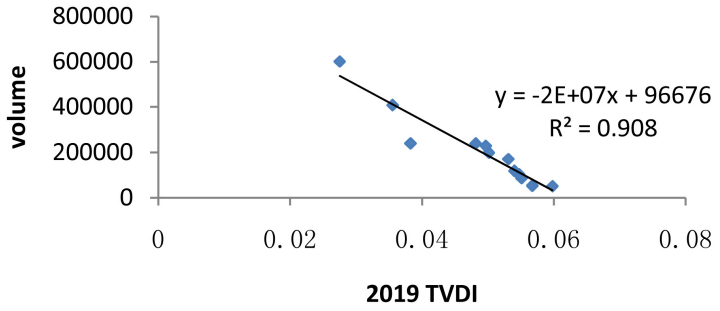

Figure 12. Relationship between TVDI and forest volume.

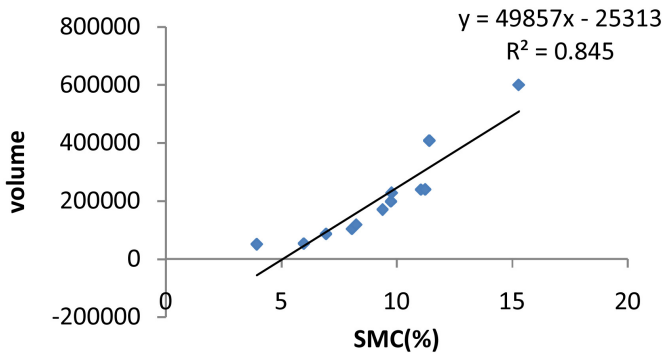

Figure 13. Relationship between SMC and forest volume.

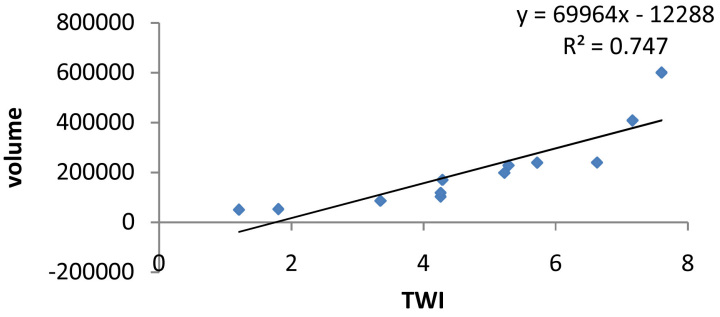

Figure 14. Relationship between TWI and forest volume.

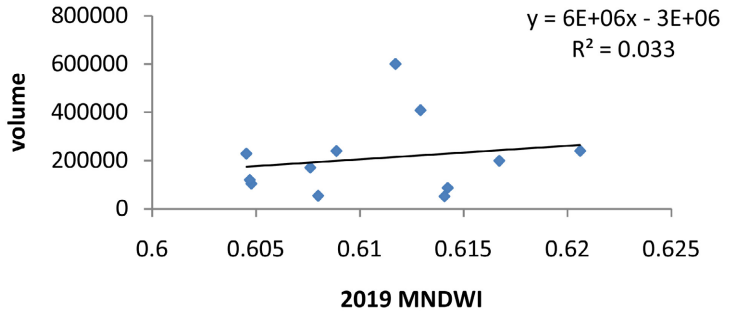

Figure 15. Relationship between MNDWI and forest volume.

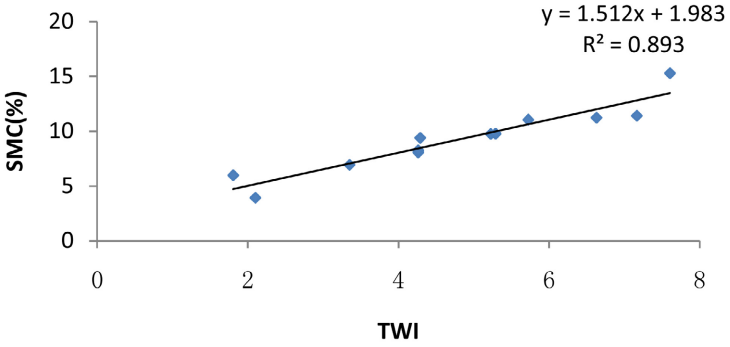

Figure 16. Relationship between TWI and SMC.

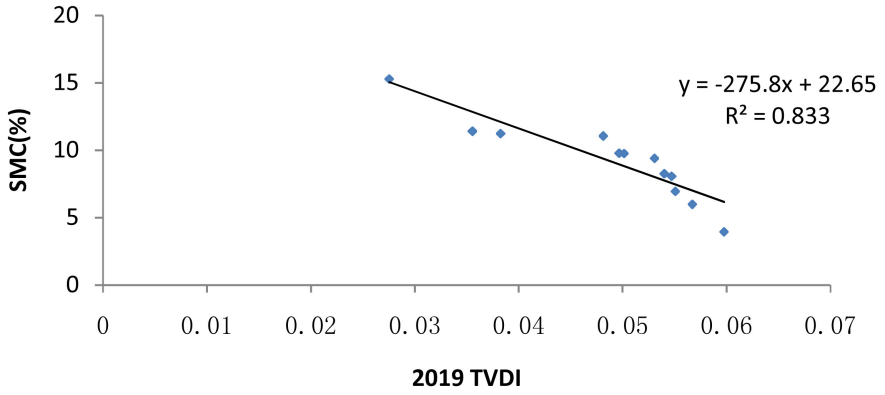

Figure 17. Relationship between SMC and TVDI.

impact of soil moisture on tree volume. They show the changes in soil moisture with respect to changes in tree volume. Soil moisture content increases with an increase in value for TWI and MNDWI while it decreases with an increase in value for TVDI. The predicted tree volume was higher in 2009 than in 2019 by about 129 m^3. The only predicted tree volume was for 2009, because of the availability of the elevation (independent variable) data for that year shown in Table 2. The prediction of tree volume using TVDI was poor while that of MNDWI was not considered since it exhibits a poor correlation value. Figure 13 and Figure 14 present the degree of similarity between soil moisture from field surface (SMC) and soil moisture derived from satellite images. The relationships were determined in SPSS with R^2 of 0.91, 0.85, 0.75 and 0.033 between volume

Table 2. Tree volume and soil moisture level.

Plot No.	Field Tree Vol. for 2019	2019		2009		TWI predicted Volume		2019 TDVI predicted Volume
		TVDI	TWI	TVDI	TWI	2019	2009	
1	50931.6	0.06	2.10	0.04	2.10	24041.4	24041.4	877961.0
2	53372.5	0.06	1.81	0.07	1.81	3439.8	3444.0	836119.0
3	86480.04	0.06	3.35	0.10	3.35	111502.7	111636.3	758833.0
4	103771.1	0.06	4.26	0.09	4.36	175231.5	182227.9	783289.0
5	118757.5	0.05	4.26	0.11	4.26	175231.5	175231.5	753151.0
6	170609.1	0.05	4.29	0.10	4.29	177059.0	177059.7	772777.0
7	198645.5	0.05	5.22	0.09	5.22	242641.1	242650.9	782315.0
8	228,425	0.05	5.29	0.60	5.29	247082.4	247058.6	847379.0
9	239,379	0.05	5.72	0.10	5.72	277442.6	277409.0	761487.0
10	239850.3	0.04	6.63	0.10	6.53	340811.8	333815.4	763831.0
11	408616.7	0.04	7.16	0.10	7.16	378311.1	378311.1	768295.0
12	600672.4	0.03	7.60	0.08	7.60	409064.5	409102.3	798989.0
13	2,499,510.7					2561859.4	2,561,988.1	9,504,426.0

and TVDI, SMC, TWI, MNDWI respectively. The results also revealed strong relationships between ground soil moisture (SMC) data and satellite-based soil moisture (TWI and TVDI) data as 0.89 between SMC and TWI and 0.83 between TVDI and SMC.

From Figures 2-11, it is obvious that the soil moisture decreased from the base year to the most recent year. The soil moisture content is highest in forested and water-logged areas (dark blue to light green) and low in bare surfaces (yellow to dark red). Figures 12-15 show the effect of soil moisture level on tree volume of the study area, and the results may not be unconnected to the lower tree volume in 2019 with lower soil moisture and higher tree volume in 2009 with higher soil moisture The soil moisture by TWI model was only produced for the year 2009 and 2019 because of the availability of field elevation data for 2019 and digital elevation image for 2009. This model gives the best prediction of tree volume in 2019 and was used to determine the tree volume status of the area in 2009 (Table 1). Presenting soil moisture distribution in form of vegetation indexes is to easily relate it with tree volume. The graphs indicate strong relationships of tree volume and soil moisture with regression values of 0.91, 0.85, and 0.75, except 0.033 with MNDWI. Check mating the activities of man as the major cause of forest degradation around and within the forest reserve would save the forest ecosystem from sounding effects of climate change like excessive evaporation, transpiration and evapotranspiration that could reduce soil water level thereby affecting tree volume.

The TWI increased along the lower surfaces, and no connection between TWI

distribution and TVDI could be detected. The TVDI values change with vegetation distribution. Areas indicated as wet by the TVDI are assigned lower vegetation class, while MNDWI increased with vegetation cover. In situ measured soil moisture did not agree well with MNDWI. This weak relationship between the index and both soil moisture and tree volume raises questions of the index validity, suitability and comparability. Here it should also be mentioned that the results are largely dependent on the actual data that were used. Higher resolutions and further variations in TWI calculation might produce different results. The TWI model was a good predictor for tree volume and soil moisture content. It can be reasoned that upslope areas are correctly identified as dry and low areas classified as wet.

The Ts/Fcd values plotted against each other, as shown in Figure 18, result in a triangle whose edges represent either dry (low canopy and low evapotranspiration) or moist (high canopy and high evapotranspiration) conditions.

The dry edge was developed from Equation (10).

$$T_s = a + b_{fcd} \tag{10}$$

Figure 11 indicates a strong relationship between SMC, which is field-based soil moisture content and tree volume. Interestingly the satellite-based soil moisture level content relates strongly with field-based soil moisture content (Figure 13 and Figure 14), and this made the prediction of tree volume possible.

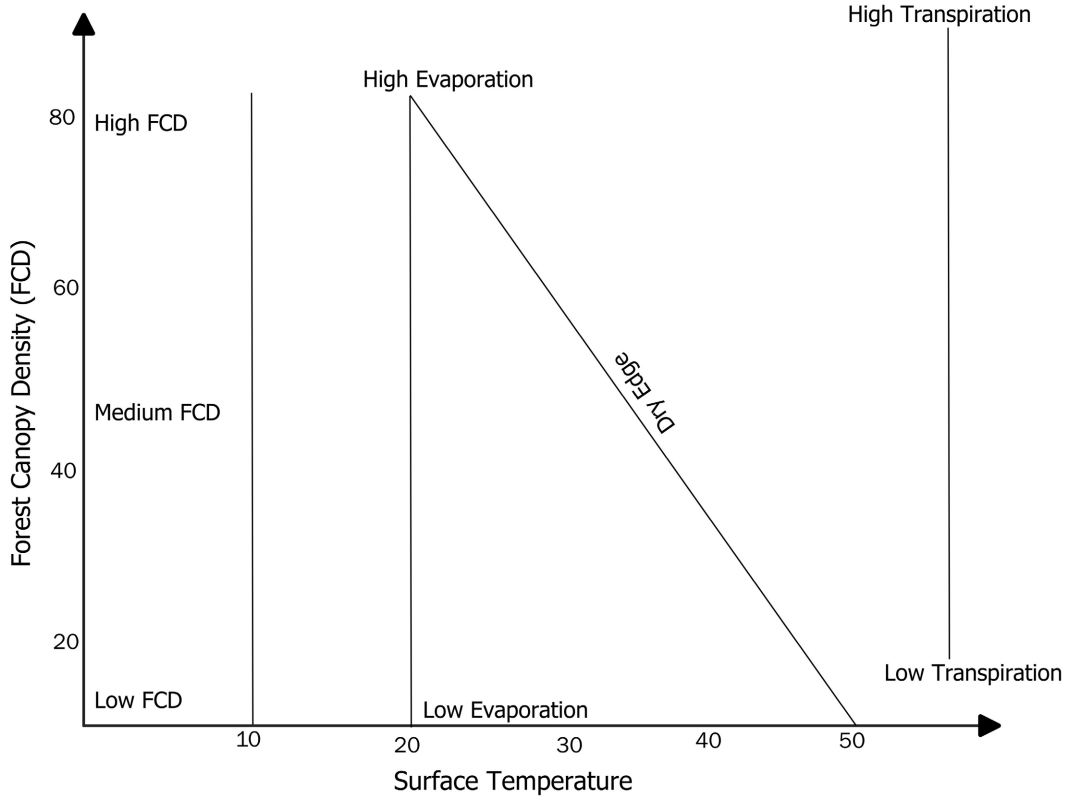

Figure 18. Simplified representation of the of Ts and Fcd relationships. (source: developed from the research results). FCD = forest canopy density.

3.2. Data Validation

The sample points were compared to the corresponding pixel values in the generated surfaces. Regressions values are shown in figures are 0.90 for TWI and 0.83 for the TVDI surface, respectively. Both correlation coefficients are rather high, although there seems to be a slightly higher correlation with the TWI surface. P-values of 0.02 for the TVDI correlation and 0.04 for the TWI correlation show that the sample size was large to achieve a statistically significant result. It is important to note that weather conditions (dry) at the time the samples were collected are similar to the ones of the satellite image acquisition date in 2019.

4. Conclusion and Recommendations

This study assessed soil moisture distribution using three different methods: Topographic Wetness Index (TWI), Temperature-Vegetation Dryness Index (TVDI) and Modified Normalized Difference Water Indexes (MNDWI) for IITA forest reserve. In-situ soil moisture was carried out and co-located to the derived moisture indices from satellite images. Index dependencies on in-situ soil moisture and tree volume were investigated and significant correlations were detected. Only MNDWI showed weak correlations with *in-situ* measured soil moisture and tree volume. However, since both TWI and TVDI indexes correlate strongly with *in-situ* measured soil moisture and that of tree volume, this suggests that both methods can be used to model soil moisture and tree volume for this area. The establishment of combined effective models for soil moisture determination over large areas requires more extensive in situ measurements and methods to fully assess the models' capabilities, limitations and value for hydrological and tree volume predictions.

Conflicts of Interest

The authors declare no conflicts of interest regarding the publication of this paper.

References

Agbor, C. F., & Makinde, E. O. (2018). Land Surface Temperature Mapping Using Geoinformation Techniques. *Geoinformatics FCE CTU, 17,* 17-32. https://doi.org/10.14311/gi.17.1.2

Agbor, C. F., Pelemo, O. J., Aigbokhan, O. J., Osudiala, C. S., & Alagbe, J. (2017). Forest Loss Assessment in South-West Nigeria Using Geospatial Technologies. *International Journal of Applied Research and Technology, 6,* 45-52.

Akindele, S. O. (1991). Development of a Site Index Equation for Teak Plantations in Southwestern Nigeria. *Journal of Tropical Forest Science, 4,* 162-169.

Alo, A. A., & Aturamu, O. (2014). Spatial Distribution of Colleges of Education and Effects on the Forest Ecosystem: A Case Study of College of Education Ikere, Nigeria. *International Journal of Research in Agricultural Sciences, 1,* 379-384.

Alo, A. A., Chukwu, O., & Ogunleye, B. C. (2017). Comparison of Four Distribution Functions for Fitting Diameter in Second Rotation *Tectona grandis* Linn. f. Plantations

in Eda Forest Reserve, Nigeria. *Forests and Forest Products Journal, 10,* 15-26.

Alo, A. A., Onyekwelu, J. C., & Akindele, S. O. (2011). Taper Equations for *Gmelina arborea* in Omo Forest Reserve, Southwestern Nigeria. *Journal of Applied Tropical Agriculture, 12,* 120-127.

Avery, T. E., & Burkhart, H. E. (1983). Forest Measurements. McGraw-Hill Publishing, New York.

Bai, X., Zhang, L., He, C., & Zhu, Y. (2020). Estimating Regional Soil Moisture Distribution Based on NDVI and Land Surface Temperature Time Series Data in the Upstream of the Heihe River Watershed, Northwest China. *Remote Sensing, 12,* Article 2414. https://doi.org/10.3390/rs12152414

Bauer, P., Gumbricht, T., & Kinzelbach, W. (2006). A Regional Coupled Surface Water/Groundwater Model of the Okavango Delta, Botswana. *Water Resources Research, 42,* W04403. https://doi.org/10.1029/2005WR004234

Briggs, L. J. (2016). *The Mechanics of Soil Moisture Paperback* (38 p). Wentworth Press.

Bryant, R., Bryant, R., Thoma, D., Moran, S., Goodrich, D., Keefer, T., Paige, G., & Skirvin, S. (2003). Evaluation of Hyperspectral, Infrared Temperature and Radar Measurements for Monitoring Surface Soil Moisture. In R. Bryant, R. Bryant, D. Thoma, S. Moran, D. Goodrich, T. Keefer, G. Paige, & Skirvin, S. (Eds.), *Proceedings of the First Interagency Conference on Research in the Watersheds* (pp. 528-533). Forgotten Books.

Carlson, T. (2007). An Overview of the "Triangle Method" for Estimating Surface Evapotranspiration and Soil Moisture from Satellite Imagery. *Sensors, 7,* 1612-1629. https://doi.org/10.3390/s7081612

Chander, G., Markham, B. L., & Helder, D. L. (2009). Summary of Current Radiometric Calibration Coefficients for Landsat MSS, TM, ETM+, and EO-1 ALI Sensors. *Remote Sensing of Environment, 113,* 893-903. https://doi.org/10.1016/j.rse.2009.01.007

Egbinola, C., & Amobichukwu, A. (2013). Climate Variation Assessment Based on Rainfall and Temperature in Ibadan, South-Western, Nigeria. *Journal of Environment and Earth Science, 3,* 32-45.

Giannini, M. B., Belfiore, O. R., Parente, C., & Santamaria, R. (2015). Land Surface Temperature from Landsat 5 TM Images: Comparison of Different Methods Using Airborne Thermal Data. *Journal of Engineering Science and Technology Review, 8.* 83-90. https://doi.org/10.25103/jestr.083.12

Gruhier, C., De Rosnay, P., Kerr, Y., Mougin, E., Ceschia, E., Calvet, J.-C., & Richaume, P. (2008). Evaluation of AMSR-E Soil Moisture Product Based on Ground Measurements over Temperate and Semi-Arid Regions. *Geophysical Research Letters, 35,* Article ID: 10405. https://doi.org/10.1029/2008GL033330

Haas, J. (2010). *Soil Moisture Modelling Using TWI and Satellite Imagery in the Stockholm Region*. Royal Institute of Technology.

Hassan, Q. K., Bourque, C. P. A., Meng, F. R., & Cox, R. M. (2007). A Wetness Index Using Terrain-Corrected Surface Temperature and Normalized Difference Vegetation Index Derived from Standard MODIS Products: An Evaluation of Its Use in a Humid Forest-Dominated Region of Eastern Canada. *Sensors, 7,* 2028-2048. https://doi.org/10.3390/s7102028

Houser, P. R., Shuttleworth, W. J., Famiglietti, J. S., Gupta, H. V., Syed, K. H., & Goodrich, D. C. (1998). Integration of Soil Moisture Remote Sensing and Hydrologic Modeling Using Data Assimilation. *Water Resources Research, 34,* 3405-3420. https://doi.org/10.1029/1998WR900001

Kimura, R. (2007). Estimation of Moisture Availability over the Liudaogou River Basin of

the Loess Plateau Using New Indices with Surface Temperature. *Journal of Arid Environments, 2,* 237-252. https://doi.org/10.1016/j.jaridenv.2006.12.021

Komeil, R., Anuar, A., Ali, S., & Sharifeh, H. (2014). Water Feature Extraction and Change Detection Using Multitemporal Landsat Imagery. *Journal name: Remote Sensing, 6*, 4173-4189. https://doi.org/10.3390/rs6054173

Makinde, E. O., & Agbor, C. F. (2019). Geoinformatic Assessment of Urban Heat Island and Land Use/Cover Processes: A Case Study from Akure. *Environmental Earth Sciences, 78,* Article No. 483. https://doi.org/10.1007/s12665-019-8433-7

Maselli, F., & Chiesi, M. (2007). Integration of Multi-Source NDVI Data for the Estimation of Mediterranean Forest Productivity. *International Journal of Remote Sensing, 27,* 55-72. https://doi.org/10.1080/01431160500329486

Milly, P., & Kabala, Z. (1985). Integrated Modeling and Remote Sensing of Soil Moisture. Hydrologic Applications of Space Technology. In Proceedings of the Cocoa Beach Workshop, Florida, August 1985. IAHS Publication No. 160.

Moran, M. S., Peters-Lidard, C. D., Watts, J. M., & McElroy, S. (2014). Estimating Soil Moisture at the Watershed Scale with Satellite-Based Radar and Land Surface Models. *Canadian Journal of Remote Sensing, 30,* 805-826. https://doi.org/10.5589/m04-043

Naira, C., Robert, L., Ramata, M., & Marouane, T. (2007). Surface Soil Moisture Status over the Mackenzie River Basin Using a Temperature/Vegetation Index. In *2007 IEEE International Geoscience and Remote Sensing Symposium* (pp. 1846-1848). IEEE. https://doi.org/10.1109/IGARSS.2007.4423182

Nemani, R., & Running, S. (1989). Estimation of Regional Surface Resistance to Evapotranspiration from NDVI and Thermal-IR AVHRR Data. *Journal of Applied Meteorology, 28*, 276-284

Onyekwelu, J., Kateb, H., Stimm, B., & Mosandi, R. (2003). Growth Characteristics and Management Scenarios for Plantation-Grown *Gmelina arborea* and *Nauclea diderrichii* in South-Western Nigeria. In R. Mosandl, H. El Kateb, & B. Stimm (Eds.), *Waldbau—Weltweit. Beiträge zur internationalen Waldbauforschungr* (pp. 147-163). Forstl. Forschungsberichte.

Price, J. C. (1990). Using Spatial Context in Satellite Data to Infer Regional Scale Evapotranspiration. *IEEE Transactions on Geoscience and Remote Sensing, 28,* 940-948. https://doi.org/10.1109/36.58983

Rokni, K., Ahmad, A., Selamat, A., & Hazini, S. (2014). Water Feature Extraction and Change Detection Using Multitemporal Landsat Imagery. *Remote Sensing, 6,* 4173-4189. https://doi.org/10.3390/rs6054173

Sandholt, I., Rasmussen, K., & Andersen, J. (2002). A Simple Interpretation of the Surface Temperature/Vegetation Index Space for Assessment of Surface Moisture Status. *Remote Sensing of Environment, 79,* 213-224. https://doi.org/10.1016/S0034-4257(01)00274-7

Seelig, H. D., Hoehn, A., Stodieck, L. S., Klaus, D. M., Adams, W. W., & Emery, W. J. (2008). The Assessment of Leaf Water Content Using Leaf Reflectance Ratios in the Visible, Near-, and Short-Wave-Infrared. *International Journal of Remote Sensing, 29,* 3701-3713. https://doi.org/10.1080/01431160701772500

Verstraeten, W. W., Veroustraete, F., Van Der Sande, C. J., Grootaers, I., & Feyen, J. (2006). Soil Moisture Retrieval Using Thermal Inertia, Determined with Visible and Thermal Spaceborne Data, Validated for European Forests. *Remote Sensing of Environment, 101,* 299-314. https://doi.org/10.1016/j.rse.2005.12.016

Wang, L., Qu, J. J., Zhang, S., Hao, X., & Dasgupta, S. (2007). Soil Moisture Estimation Using MODIS and Ground Measurements in Eastern China. *International Journal of*

Remote Sensing, 28, 1413-1418. https://doi.org/10.1080/01431160601075525

Xu, B. C., Gichuki, P., Shan, L., & Li, F. M. (2006). Aboveground Biomass Production and Soil Water Dynamics of Four Leguminous Forages in Semiarid Region, Northwest China. *South African Journal of Botany, 72,* 507-516. https://doi.org/10.1016/j.sajb.2006.01.005

Zeng, Y., Feng, Z., & Xiang, N. (2004). Assessment of Soil Moisture Using Landsat ETM+ Temperature/Vegetation Index in Semiarid Environment. *International Geoscience and Remote Sensing Symposium (IGARSS), 6,* 4306-4309.

Zhang, F. X., Gao, Z. Q., & Zuo , L. J. (2007). Study on Relationship of Soil Moisture and Land Cover: A Case in Lijin County, Shandong Province. *Remote Sensing and Modeling of Ecosystems for Sustainability IV, 6679,* 379-386. https://doi.org/10.1117/12.727766

Zwartendijk, B. W., Van Meerveld, H. J., Ghimire, C. P., Bruijnzeel, L. A., Ravelona, M., & Jones, J. P. G. (2017). Rebuilding Soil Hydrological Functioning after Swidden Agriculture in Eastern Madagascar. *Agriculture, Ecosystems & Environment, 239,* 101-111. https://doi.org/10.1016/j.agee.2017.01.002